Introduction

The use of 3D printing to create rock replicas for studying of rocks geomechanical and seepage characteristics has become increasingly popular. Replicas are used to study the transport characteristics of pore channels and fractures of various shapes and sizes under static no load conditions [Li et al., 2021; Wu et al., 2022], but the use of replicas in studying seepage in pore channels under cyclic loading, is limited, although it could bring new data to the study of seepage laws. This paper presents a method for producing replicas of porous rock analogues and comparative filtration studies of porous, fractured rock samples and their replicas under cyclic loading.

Method

The application of 3D printing in filtration studies is currently constrained by resolution limitations, which impede the accurate representation of complex pore structures. Furthermore, the removal of residual resin from printed porous media, particularly those with low porosity, presents a significant challenge, often leading to pore space distortion and subsequently impacting filtration performance. To address these challenges, certain academic inquiries advocate for the substitution of porous media with solid models incorporating a conducting channel, exemplified by configurations such as spiral geometries [Ibrahim et al., 2021] or fracture-like structures [Wu et al., 2022]. This approach facilitates greater control over channel geometry and purity of experimental conditions. The research methodology employed in this study involved the implementation of cyclic loading on 3D printed replicas, featuring grooves of varying dimensions positioned centrally within the samples. The workflow, encompassing model generation, printing process, and the final replicas, is illustrated in Figure 1. Initially, a digital 3D model representing one half of the sample, featuring a central groove (Figure 1a), was created alongside a complementary half lacking the groove. To mitigate the influence of light scattering during printing and ensure dimensional accuracy, a rectangular groove profile was chosen (Figure 1b). Samples were printed on supports with the groove oriented towards the display (Figure 1c), a configuration designed to optimize printing quality in the critical groove region. Comparative filtration tests were also conducted on rock samples: porous sandstone and impermeable silicified dolomite, artificially split in half.

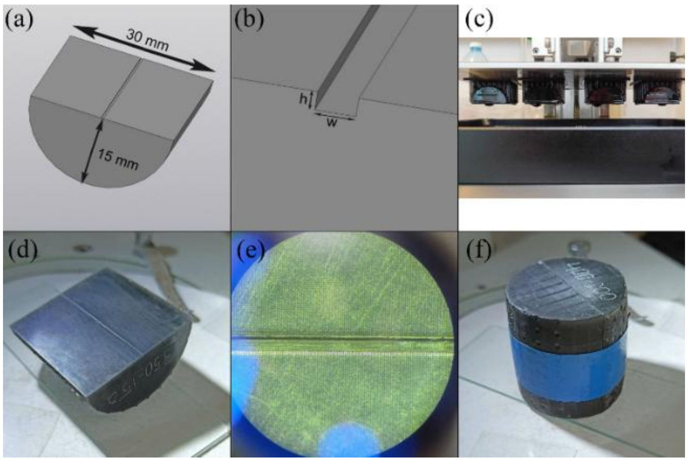

Figure 1 *Replicas fabrication: a – shape and size of the core half; b – shape of the groove; c – printing; g – the printed half; d – view of the groove under a microscope; e – replica assembled from two halves.*

After printing, the replicas were examined for surface smoothness (Figure 1d) and groove cleanliness (Figure 1e). Then the two halves, with and without a groove, were joined together (Figure 1a) and the sample was placed in the core holder of the UltraPoroPerm-500 installation. Filtration was carried out with a constant nitrogen flow rate and cyclic confining pressure. More details on the research methodology can be found in [Kozhevnikov et al., 2023]. The conductivity of the replica was determined by the formula:

$$C = Q \Big/ \frac{(P_{in}^2 - P_o^2)}{P_o \cdot L}$$

where Q is the nitrogen flow rate, cm^3/s; P_{in} is the nitrogen injection pressure, Pa; P_o is the pressure at the sample outlet, Pa; L is the sample length (mm).

Results and discussion

Comparative conductivity test results for replica with a 350x150 μm groove and rock samples are shown in the graph (Figure 2). It was found that the conductivity dynamics of the replica is identical to that of a real porous and artificially split sample. A closer look (Figure 2d,e,f) shows that with increasing confining pressure, the conductivity of the replica and rock decreases equally, first a sharp drop, and then a smooth creeping decrease in conductivity. A smoother line of conductivity dynamics is found in sample with an artificial crack, that also has the largest amplitude of conductivity change under cyclic loading (Figure 2e, h). Porous samples have a larger spread in conductivity dynamics, which is due to a large number of pores and microcracks of changing geometry during creep. Replicas combine a fairly high smoothness of conductivity dynamics inherent in artificial cracks and a spread in conductivity dynamics, as in porous samples. Creep in the replica and in the sample with an artificial crack is caused by the sliding of the two halves relative to each other, and in the porous sandstone sample – due to the sliding of microcracks. This behavior confirms the presence of relaxation microcracks in the porous sandstone, which were induced by its extraction from a depth of 1800 m during drilling of an oil well. When the confining pressure decreases (Figure 2g,h,i), in all samples the conductivity is restored first instantly, and then in a creeping mode. In the artificially split sample, the conductivity recovery curve is smooth (Figure 2h). In the replica and in the porous sandstone sample, when unloading, the conductivity curve exhibits a broken shape, reflecting the restoration of conductivity due to the intermittent sliding of the surfaces of the halves and microcracks during the recovery of the sample's shape [Karev et al., 2021; Riabokon et al., 2023].

The conductivity of both replicas and rock samples under confining pressure is well described by the classical power equation ($R^2 = 0.99$) as shown in Figure 3 [Kozhevnikov et al., 2023; Yue et al., 2024]. It was also observed that replicas exhibit less permeability hysteresis in each loading cycle compared to the rock samples. For replicas, the conductivity curves remain parallel during both loading and unloading phases. The exponents of the power equations that describe the changes in conductivity of replicas during loading and unloading are slightly different, with values of -0.282 and -0.266, respectively (Figure 3c). The sample with an artificial crack demonstrates a significant decrease in conductivity during the first loading cycle, but in subsequent cycles, the conductivity curves during loading and unloading become parallel. The exponents of the power equations describing the change in conductivity of the sample with an artificial crack during loading and unloading are nearly identical, with values of -1.3 and -1.31, respectively (Figure 3b). In sandstone samples, permeability hysteresis is more pronounced. The exponents of the power equations for these samples under loading and unloading conditions are -0.133 and -0.085, respectively.

Conclusions

Thus, based on the comparative analysis, it was established that the application of 3D printing technology can be used in geomechanical studies, in particular in the study of the effect of cyclic deformations on the conductivity of thin capillaries, which can serve as analogs of porous medium channels. The use of replicas in the study of flow modes allows one to avoid the influence of extraneous factors, such as permeability hysteresis, colloid migration, etc. Also, with the help of 3D printing, it is possible to create channels with different configurations, which will allow more accurately establishing the seepage laws in porous and fractured media.

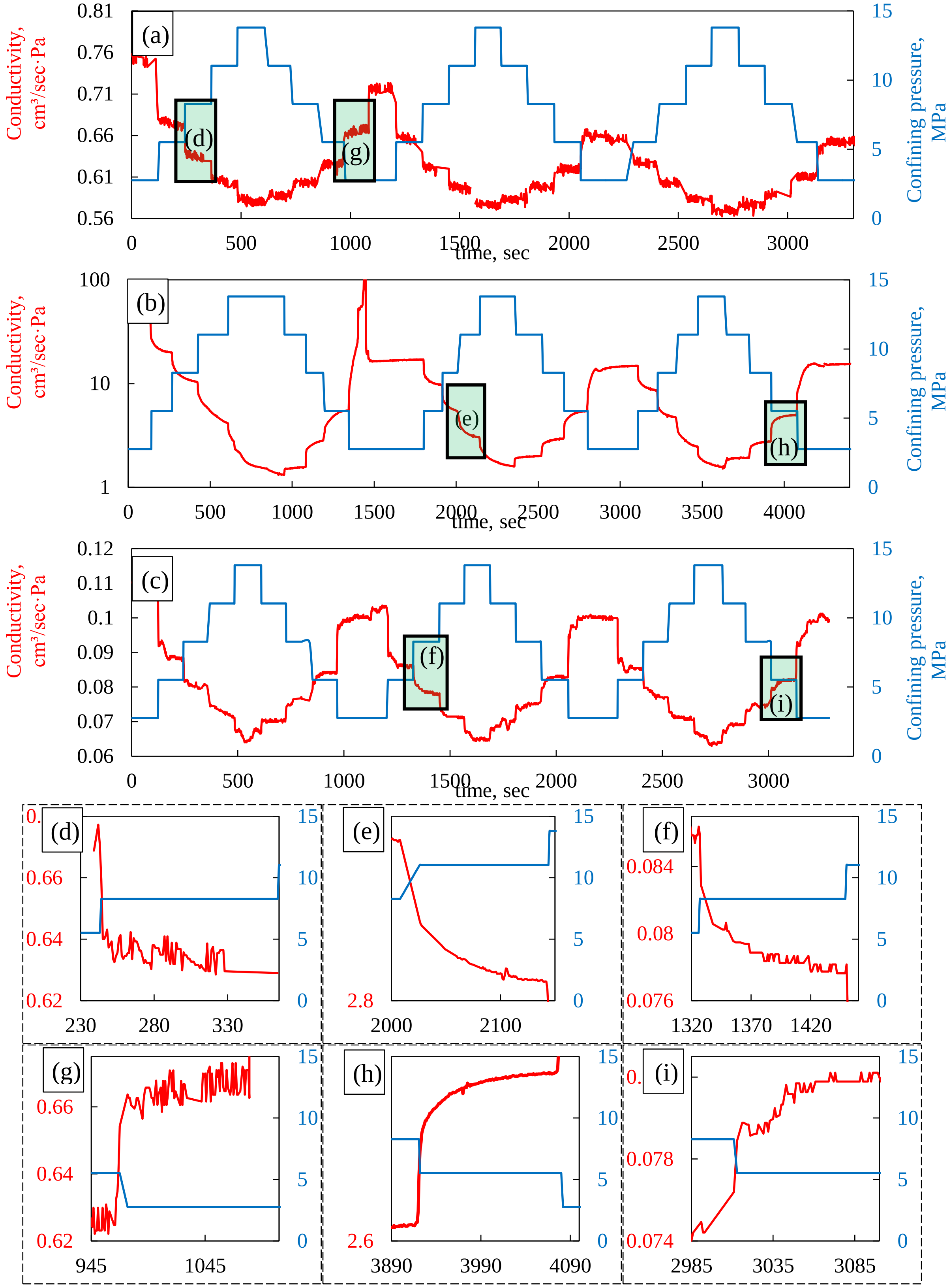

Figure 2 *Dynamics of conductivity of a porous sandstone sample (a, d, g), an impermeable sample with an artificial crack (b, e, h) and a replica with a groove size of 350x150 μm (c, f, i) under cyclic loading. The red line is conductivity, the blue line is the confining pressure.*

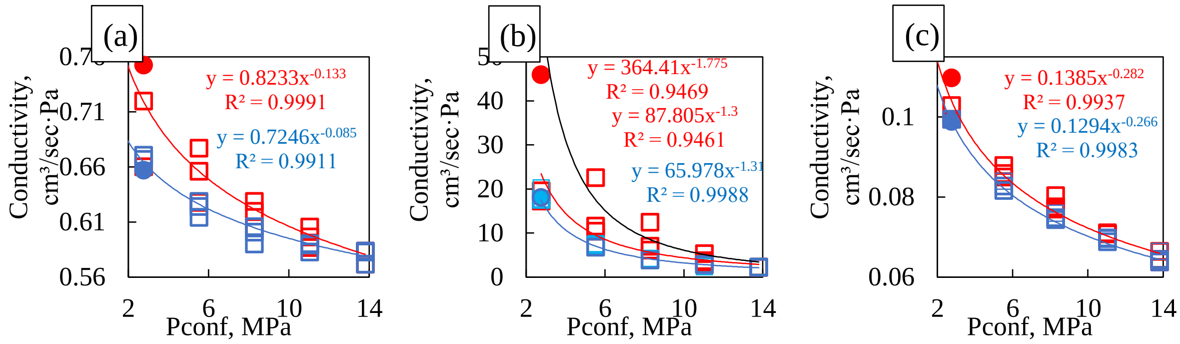

***Figure 3** Conductivity of a porous sandstone sample (a), a sample with an artificial crack (b) and a replica with a groove size of 350x150 μm (c) from the confining pressure. Red symbols correspond to the loading path, blue symbols - to the unloading path. Solid red and blue dots are the initial and final conductivity, respectively. Solid lines are approximations.*

Acknowledgements: This research was funded by the RUSSIAN SCIENCE FOUNDATION project no. 23-19-00699, https://rscf.ru/project/23-19-00699/

References

Ibrahim, E. R., Jouini, M. S., Bouchaala, F., and Gomes, J. [2021]. Simulation and Validation of Porosity and Permeability of Synthetic and Real Rock Models Using Three-Dimensional Printing and Digital Rock Physics. *ACS Omega*, *6*(47), 31775–31781. https://doi.org/10.1021/acsomega.1c04429

Karev, V. I., Khimulia, V. V., and Shevtsov, N. I. [2021]. Experimental Studies of the Deformation, Destruction and Filtration in Rocks: A Review. *Mechanics of Solids*, *56*(5), 613–630. https://doi.org/10.3103/S0025654421050125

Kozhevnikov, E. V., Turbakov, M. S., Riabokon, E. P., and Gladkikh, E. A. [2023]. Apparent Permeability Evolution Due to Colloid Migration Under Cyclic Confining Pressure: On the Example of Porous Limestone. *Transport in Porous Media*. https://doi.org/10.1007/s11242-023-01979-5

Kozhevnikov, E. V., Turbakov, M. S., Riabokon, E. P., Gladkikh, E. A., and Poplygin, V. V. [2023]. Cyclic confining pressure and rock permeability: Mechanical compaction or fines migration. *Heliyon*, *9*(11), e21600. https://doi.org/10.1016/j.heliyon.2023.e21600

Li, B., Wang, J., Liu, R., and Jiang, Y. [2021]. Nonlinear fluid flow through three-dimensional rough fracture networks: Insights from 3D-printing, CT-scanning, and high-resolution numerical simulations. *Journal of Rock Mechanics and Geotechnical Engineering*, *13*(5), 1020–1032. https://doi.org/10.1016/j.jrmge.2021.04.007

Riabokon, E., Gladkikh, E., Turbakov, M., Kozhevnikov, E., Guzev, M., Popov, N., and Kamenev, P. [2023]. Effects of ultrasonic oscillations on permeability of rocks during the paraffinic oil flow. *Géotechnique Letters*, *13*(3), 1–20. https://doi.org/10.1680/jgele.22.00137

Wu, H., Ju, Y., Han, X., Ren, Z., Sun, Y., Zhang, Y., and Han, T. [2022]. Size effects in the uniaxial compressive properties of 3D printed models of rocks: an experimental investigation. *International Journal of Coal Science & Technology*, *9*(1), 83. https://doi.org/10.1007/s40789-022-00556-3

Yue, L., Li, W., Liu, Y., Li, S., and Wang, J. [2024]. A review of mechanical deformation and seepage mechanism of rock with filled joints. *Deep Underground Science and Engineering*. https://doi.org/10.1002/dug2.12126